Investigation of the local composition enhancement and related dynamics in supercritical CO_2-cosolvent mixtures via computer simulation: The case of ethanol in CO_2

Ioannis Skarmoutsos, Dimitris Dellis, and Jannis Samios[a)]
Laboratory of Physical Chemistry, Department of Chemistry, University of Athens, Panepistimiopolis 157-71, Athens, Greece

(Received 10 January 2007; accepted 18 April 2007; published online 11 June 2007)

The supercritical mixture ethanol-carbon dioxide (EtOH–CO_2) with mole fraction of ethanol $X_{EtOH} \cong 0.1$ was investigated at 348 K, by employing the molecular dynamics simulation technique in the canonical ensemble. The local intermolecular structure of the fluid was studied in terms of the calculated appropriate pair radial distribution functions. The estimated average local coordination numbers and mole fractions around the species in the mixture reveal the existence of local composition enhancement of ethanol around the ethanol molecules. This finding indicates the nonideal mixing behavior of the mixture due to the existence of aggregation between the ethanol molecules. Furthermore, the local environment redistribution dynamics have been explored by analyzing the time correlation functions (TCFs) of the total local coordination number (solvent, cosolvent) around the cosolvent molecules in appropriate parts. The analysis of these total TCFs in the auto-(solvent-solvent, cosolvent-cosolvent) and cross-(solvent-cosolvent, cosolvent-solvent) TCFs has shown that the time dependent redistribution process of the first solvation shell of ethanol is mainly determined by the redistribution of the CO_2 solvent molecules. These results might be explained on the basis of the CO_2–CO_2 and EtOH–CO_2 intermolecular forces, which are sufficiently weaker in comparison to the EtOH–EtOH hydrogen bonding interactions, creating in this way a significantly faster redistribution of the CO_2 molecules in comparison with EtOH. Finally, the self-diffusion coefficients and the single reorientational dynamics of both the cosolvent and solvent species in the mixture have been predicted and discussed in relationship with the local environment around the species, which in the case of the EtOH molecules seem to be strongly affected. © *2007 American Institute of Physics*. [DOI: 10.1063/1.2738476]

I. INTRODUCTION

In recent years, the properties of supercritical (sc) "green" solvents have been the subject of major interest for many research groups due to their efficiency to replace toxic organic solvents and their ability to act as intermediates in many important chemical industrial processes.[1–7] We mention for instance that their dissolving power could be adjusted by slightly varying the pressure, tuning by this way allows selection of the solubility of different types of solutes in these fluids.

Among various types of sc solvents, the nontoxic and nonflammable $scCO_2$, with a near-ambient critical temperature of 304.13 K, appears to be extremely popular in several chemical processes that take place at mild, and hence more cost-efficient, conditions. Note, however, that the use of $scCO_2$ as solvent has some serious limitations in the case of the dissolution of polar organic compounds. According to the literature, the solubility of polar organic solutes in pure $scCO_2$ is quite restricted and decreases with increasing the solute polarity.[7–14] On the other hand, previous experimental studies have revealed that this difficulty can be overcome by adding small amounts of polar cosolvents in $scCO_2$. Further to this, a proper choice of the cosolvent used may control the selectivity and dissolution of specific polar compounds, making thus the CO_2-cosolvent systems extremely useful in extraction processes. As a result, all these features make the CO_2-cosolvent mixtures promising and attractive alternatives to liquid and pure sc solvents in separation techniques (sc chromatography, industrial waste treatment, etc.).[15,16]

Among several types of polar cosolvents, the lower alcohols (methanol, ethanol, 2-propanol, etc.) have been widely used for all the aforementioned purposes. The alcohol cosolvents are extremely important, since they enhance significantly the solubility of pharmaceutical (anti-inflammatory) drugs[17] in $scCO_2$, as well as their use has been also emerged as potential method for achieving pollution-free dyeing.[18] Moreover, the CO_2-ethanol mixed solvent has been used in several important applications of materials science, such as polymer fractionation, fine particle synthesis, etc.[7,19,20]

According to several experimental studies, when a polar compound dissolves in a $scCO_2$-alcohol mixture, the local mole fraction of the alcohol cosolvent around the polar solute is enhanced.[21–24] This phenomenon is often called as *local composition enhancement* (LCE) and probably might be the main determinant concerning the whole evolution of the

[a)]Author to whom correspondence should be addressed. Electronic mail: isamios@chem.uoa.gr

solvation processes of polar solutes in these mixed solvents. In other words, if one assumes that such LCE effects are closely related to the formation of local aggregates constructed by the alcohol molecules in the mixed solvent, then it is reliable to consider that the polar solutes approach energetically easier the polar alcohol aggregates and become more easily dissolved. However, such a hypothesis is based only on a pure qualitative explanation of thermodynamic measurements. Note that the experimental and theoretical studies concerning the properties of the alcohol-CO_2 sc mixed solvents and especially the existence of aggregates among the alcohol molecules in these sc mixtures are very limited.[25]

According to previous molecular dynamics (MD) simulation studies of $scCO_2$–MeOH mixtures performed by our group[25] (with mole fraction of MeOH $\cong 0.1$) the MeOH molecules tend to form aggregates in the mixture by forming hydrogen bonds among them. This fact indicates that the local composition of MeOH around the MeOH (methanol) molecules is probably enhanced in the mixture. This has been also observed along the vapor-liquid coexistence curve, from the Monte Carlo (MC) simulations of Stubbs and Siepmann[26(a)] and the very recently reported MD simulations of Li and Maroncelli.[26(b)] Furthermore, our previous studies have revealed that these aggregation effects among the MeOH influence strongly the single translational dynamics of the MeOH molecules, something which was in agreement with previous experimental nuclear magnetic resonance (NMR) studies.[27]

Although a small number of experimental studies devoted to the properties of $scCO_2$–MeOH mixtures at the composition range $X_{MeOH} \cong 0.01-0.11$ have been published up to now,[25–35] thorough investigations of the properties of $scCO_2$–EtOH (ethanol) binary mixtures are scarce and most of them correspond mainly to dilute concentrations of ethanol.[30,36–41]

Therefore, the main objective of this study is to provide some information concerning the local intermolecular structure and related dynamics for the $scCO_2$–EtOH binary mixtures at about 10% molar concentrations of ethanol and especially to seek for the existence of possible LCE effects around the ethanol cosolvent molecules. In view of the great scientific and technological potentials of this mixed solvent, a deeper and quantitative understanding of the aforementioned effects becomes indispensable in order to elucidate fundamental aspects of this particularly interesting molecular system. This work is a part of our theoretical investigations on the properties of supercritical solvents[25,42–47,55] and with this effort we would like to cover this gap by providing some quantitative information concerning these particular properties of this $scCO_2$-cosolvent mixture.

II. METHODOLOGY—COMPUTATIONAL DETAILS

As mentioned in Sec. I, we are concerned with the problem of LCE and related dynamics in the binary sc mixture EtOH–CO_2. Before proceeding any further, it is necessary to present the methodology employed to estimate the properties under investigation.

In order to extract information about the local structure and composition around the solvent and cosolvent molecules in the mixture, we have calculated the local mole fractions of both species around the solvent and cosolvent molecules as a function of the distance from them, respectively, by using Eq. (1).

$$X_{ij}(r) = \frac{n_{ij}(r)}{n_{ij}(r) + n_{ii}(r)}. \tag{1}$$

In Eq. (1), $n_{ij}(r)$ denotes the corresponding local coordination numbers of the j molecules around a central i molecule (solvent or cosolvent) which are evaluated from the following integral relation:

$$n_{ij}(r) = \rho_j \int_0^r 4\pi R^2 g_{ij}(R) dR, \tag{2}$$

where ρ_j is the number density of molecules j in the mixture and $g_{ij}(r)$ the corresponding center of mass (COM) pair radial distribution function (PRDF). To denote the cosolvent (EtOH) molecules and the solvent (CO_2) ones, we will use hereafter the index "1" and "2" for EtOH and CO_2, respectively.

In order to investigate the time dependent distribution of the local environment around the cosolvent (or solvent) molecules we have defined the instantaneous local coordination number deviation $\delta n_{ij}(t)$, relative to the mean local one as $\delta n_{ij}(t) = n_{ij}(t) - \langle n_{ij} \rangle$, for a fixed cutoff distance that specifies the volume of the solvation shell around a particle. In our treatment we have used as a cutoff distance the radius that corresponds to the first minimum of the EtOH–CO_2 COM PRDF $g_{12}(r)$. The dynamics of this quantity can be calculated in terms of its autocorrelation function (ACF),

$$C_{\delta n_{ij}-\delta n_{ij}}(t) = \langle \delta n_{ij}(0)\, \delta n_{ij}(t) \rangle, \tag{3}$$

or the normalized expression,

$$C_{\delta n_{ij}-\delta n_{ij}}(t)(\text{norm}) = \frac{\langle \delta n_{ij}(0)\, \delta n_{ij}(t) \rangle}{\langle [\delta n_{ij}(0)]^2 \rangle}. \tag{4}$$

It is also possible to estimate the corresponding correlation time $\tau_{\delta n_{ij}-\delta n_{ij}}$ as

$$\tau_{\delta n_{ij}-\delta n_{ij}} = \int_0^\infty C_{\delta n_{ij}-\delta n_{ij}}(t)(\text{norm}) dt. \tag{5}$$

In the case of the solvation shell of EtOH, the average total coordination number can be expressed as a sum of two coordination numbers,

$$n_{\text{tot}(1)}(t) = n_{11}(t) + n_{12}(t), \tag{6}$$

while the local coordination number deviation can be expressed as follows:

$$\begin{aligned} \delta n_{\text{tot}(1)}(t) &= n_{\text{tot}(1)}(t) - \langle n_{\text{tot}(1)} \rangle \\ &= n_{11}(t) - \langle n_{11} \rangle + n_{12}(t) - \langle n_{12} \rangle \\ &= \delta n_{11}(t) + \delta n_{12}(t). \end{aligned} \tag{7}$$

The corresponding ACF of this quantity can be expressed by the following equation:

$$C_{\delta n_{\mathrm{tot}(1)}}(t) = \langle \delta n_{11}(0)\delta n_{11}(t)\rangle + \langle \delta n_{12}(0)\delta n_{12}(t)\rangle + \langle \delta n_{11}(0)\delta n_{12}(t)\rangle + \langle \delta n_{12}(0)\delta n_{11}(t)\rangle, \quad (8)$$

or alternatively by

$$C_{\delta n_{\mathrm{tot}(1)}}(t) = C_{\delta n_{11}-\delta n_{11}}(t) + C_{\delta n_{12}-\delta n_{12}}(t) + C_{\delta n_{11}-\delta n_{12}}(t) + C_{\delta n_{12}-\delta n_{11}}(t). \quad (9)$$

The corresponding (total) normalized ACF is given by

$$C_{\delta n_{\mathrm{tot}(1)}}(t)(\mathrm{norm}) = \frac{C_{\delta n_{11}-\delta n_{11}}(t)}{C_{\delta n_{\mathrm{tot}(1)}}(0)} + \frac{C_{\delta n_{12}-\delta n_{12}}(t)}{C_{\delta n_{\mathrm{tot}(1)}}(0)} + \frac{C_{\delta n_{11}-\delta n_{12}}(t)}{C_{\delta n_{\mathrm{tot}(1)}}(0)} + \frac{C_{\delta n_{12}-\delta n_{11}}(t)}{C_{\delta n_{\mathrm{tot}(1)}}(0)}. \quad (10)$$

From Eqs. (8)–(10), we can clearly see that this ACF can be expressed as a sum of two ACFs and two cross-correlation functions (CCF). Therefore, the time dependent distribution of the local environment around a central EtOH molecule seems to be a quite complex collective dynamical process. It is clearly even more complex in comparison with the time dependent redistribution of the local environment around a particle in pure fluids, systematically investigated in our own previous studies concerning the local density inhomogeneities and corresponding dynamics in pure sc water,[42] $scCO_2$,[55] and scMeOH,[55] as well as in a two-dimensional MD simulation study of a pure model monatomic fluid by Maddox *et al.*[48]

In this study, we performed a *NVT*-MD simulation for a system consisting of 48 ethanol and 452 CO_2 molecules in the central simulation box using standard periodic boundary conditions at sc conditions (T=348 K, P=15.87 MPa, ρ =0.611 g/cm^3) (Ref. 37) corresponding to about a 0.9 mass fraction of CO_2. We mention that previous configurational-biased MC studies in the Gibbs ensemble for the EtOH–CO_2 mixture have revealed that the system size effects, for this particular total number of simulated molecules, have been found to be negligible.[49] Note that, according to previous experimental studies the critical temperature of the mixture at this particular composition was estimated to be about 326 K,[37,38,50,51] therefore the investigated state point belongs to the supercritical phase region.

The intermolecular interactions are represented as pairwise additive with site-site Lennard-Jones (LJ) plus coulomb interactions due the quadrupole moment of CO_2 and the dipole moment of EtOH molecules. For unlike interaction sites, the Lorentz-Berthelot combining rules were used. The elementary physical potential model EPM2 was employed to describe the site-site interactions of CO_2,[52] whereas the flexible OPLS-UA one for EtOH.[53] In this potential model, the intramolecular torsion around the central C_2–O bond has been expressed by using the following potential function:

$$U(\varphi) = U_0 + \tfrac{1}{2}U_1(1+\cos\varphi) + \tfrac{1}{2}U_2(1-\cos 2\varphi) + \tfrac{1}{2}U_3(1+\cos 3\varphi). \quad (11)$$

Note that these models have been used in earlier successful simulations of both neat systems at liquid and sc conditions[45,54,55] as well as in CS studies of scMeOH–CO_2 mixture[25] and other binary sc mixtures.[43]

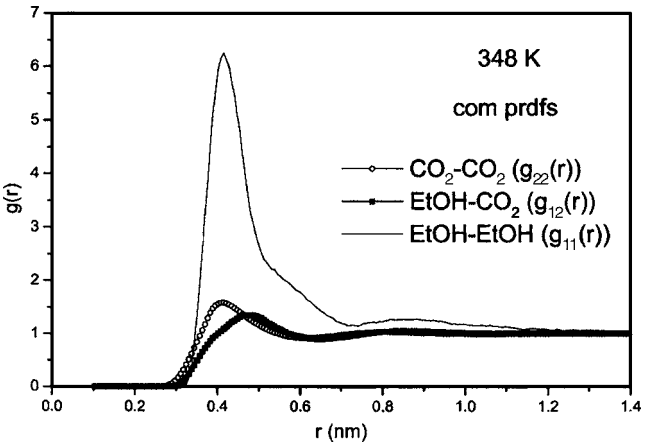

FIG. 1. The calculated CO_2–CO_2, EtOH–CO_2, and EtOH–EtOH COM PRDFs.

Note that, to achieve equilibrium of the simulated system, the MD run was extended to at least 300 ps followed by 400 ps trajectory over which the structural and dynamic properties were calculated. The integration time step was chosen to be 1 fs. The equations of motion were integrated using a leapfrog-type Verlet algorithm and the Berendsen thermostat,[56] with a temperature relaxation of 0.5 ps, was also used. In addition, the intramolecular geometry of the species was constrained during simulations by using the SHAKE method.[57] The cutoff radius of 1.2 nm was used to all LJ interactions and long-range corrections have been taken into account. Moreover, the Ewald summation technique, with the use of the more exact approximation Newton-Gregory forward difference interpolation scheme,[58,59] was applied to account for the long-range electrostatic interactions.

III. RESULTS AND DISCUSSION

A. Static intermolecular structure

The intermolecular structure of the mixture was studied on the basis of the COM and site-site PRDFS. The CO_2–CO_2, EtOH–CO_2, and EtOH–EtOH PRDFs are presented in Fig. 1, whereas the most important site-site correlations are in Figs. 2 and 3. From Fig. 1 we may observe that the EtOH–EtOH COM, PRDF exhibits a strong first maximum of 6.25 located at 0.42 nm, followed by a first minimum located at 0.74 nm. On the other hand, the first maximum for the CO_2–CO_2 PRDF is 1.58 located also at 0.42 nm, whereas that for the EtOH–CO_2 PRDF is 1.35 located at 0.47 nm. The first minimum of CO_2–CO_2 and EtOH–CO_2 COM PRDFs is located at 0.62 and 0.64 nm, respectively.

The significantly smaller first peak values obtained for the CO_2–CO_2 and EtOH–CO_2 PRDFs compared to the EtOH–EtOH one reveals a quite stronger correlation among the EtOH molecules in the mixture. The shape of the site-site EtOH–EtOH PRDFs further supports this finding, especially the O–H, O–O, and H–H functions, which are highly structured at relatively very short distances. From Fig. 2(a), the

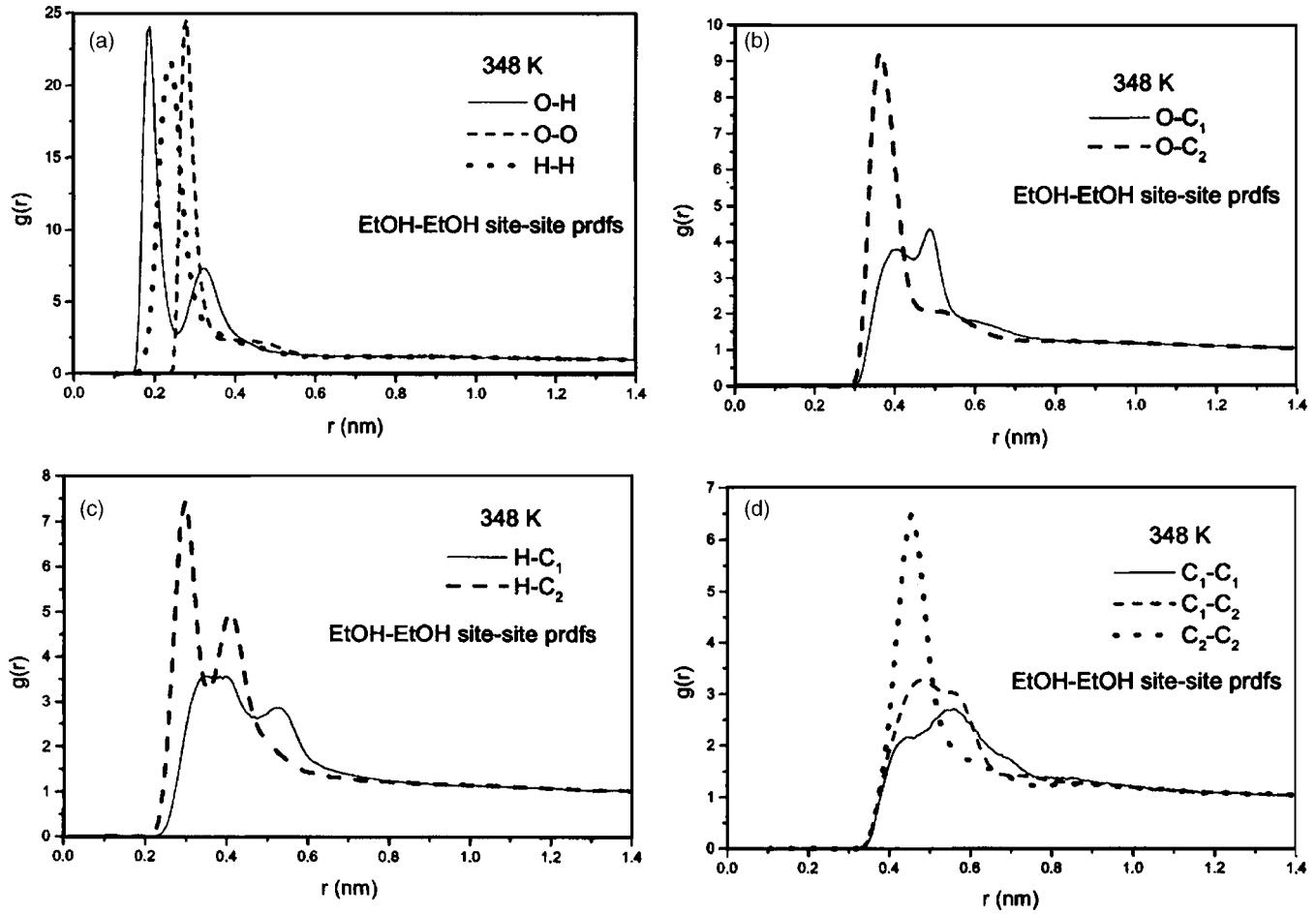

FIG. 2. The calculated EtOH–EtOH site-site PRDFs.

O–H PRDF exhibits a very sharp-peaked first maximum with amplitude of 24.1 at 0.19 nm. The corresponding first maximum values of the O–O and H–H PRDFs are 24.6 and 21.7 located at 0.28 and 0.24 nm, respectively. Such features clearly indicate the existence of hydrogen bonding (HB) among the EtOH cosolvent molecules in the mixture. It should be mentioned here that similar conclusions have been already reported for $scCO_2$–MeOH binary mixtures by our group[25] and Pfund *et al.*,[29] as well as by Stubbs and Siepmann[26(a)] along the vapor-liquid coexistence curve of the mixture, and quite recently by Li and Maroncelli.[26(b)]

Further to this, the Fourier transform infrared measurements of sc alcohol-CO_2 binary mixtures with alcohol molar concentrations up to 0.1 reported by Fulton *et al.*[30] have revealed the formation of HB aggregates among EtOH molecules, a result that is in agreement with our findings. Fulton *et al.*[30] have also proposed that the degree of HB between the alcohol molecules increases by increasing the alcohol mole fraction and probably a weak alcohol-CO_2 complex is formed in these mixtures. Similar results have been also reported in previous NMR (Ref. 32) and IR (Ref. 36) studies of dilute EtOH–CO_2 mixtures, supported further by *ab initio* calculations[36] on the EtOH–CO_2 dimer.

It is very interesting to note that according to the aforementioned *ab initio* studies, the intermolecular distance O(EtOH)$\cdots$C(CO_2) for the most energetically favorable dimer geometrical configuration has been estimated to be about 0.275 nm.[36] By inspecting carefully the O(EtOH)$\cdots$C(CO_2) site-site PRDF [Fig. 3(c)] obtained in the framework of our study, we may observe that this function exhibits a well-defined shoulder located at about 0.29 nm. This result clearly indicates some weak correlation between O(EtOH) and C(CO_2) which might lead to the stabilization of such kind of dimer configuration, as the previous *ab initio* and IR studies have also proposed.

This weak EtOH–CO_2 complex structure might be also supported by the shapes at very short distances of the H–O, H–C, and O–O site-site PRDFs depicted in Fig. 3(a).

To investigate further the existence (or not) of the ethanol aggregates in the mixture, we have also calculated the local mole fractions around the cosolvent and solvent species by using Eqs. (1) and (2). The local mole fractions of EtOH and CO_2 around each of them in the mixture are presented in Figs. 4(a) and 4(b) as a function of the intermolecular distance. Figure 4(a) shows clearly the existence of LCE of EtOH around the EtOH molecules, since at very short intermolecular distances the local mole fraction of EtOH around the EtOH molecules exhibits values significantly greater than the bulk ones. At a distance of 0.49 nm, for instance, the local mole fraction $X_{\mathrm{EtOH-EtOH}}$ is about 0.34, in other words 3.4 times greater than its bulk value. Note that the local mole fractions around the cosolvent EtOH molecules tend to reach their bulk values at relatively large intermolecular distances,

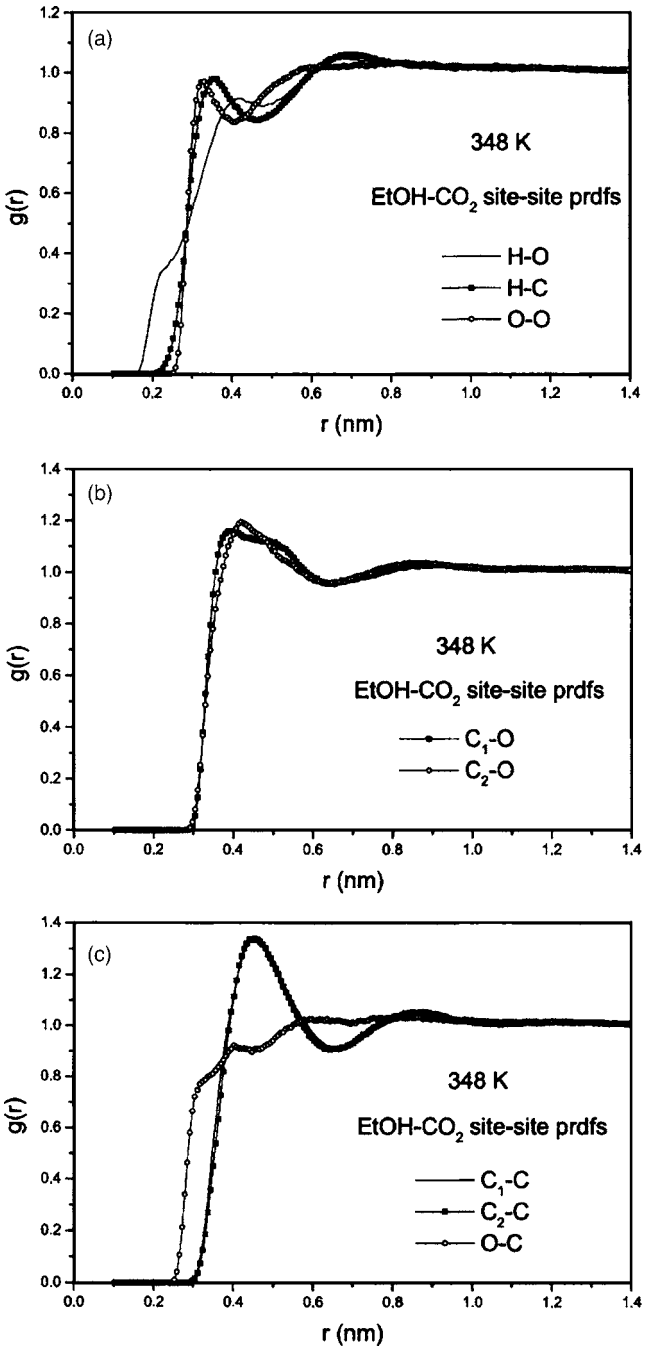

FIG. 3. The calculated EtOH–CO_2 site-site PRDFs.

up to about 1.4 nm. These results indicate the existence of strong LCE effects around the EtOH molecules and reveal the existence of EtOH aggregates in the mixture. In contrast, Fig. 4(b) shows that around the CO_2 molecules such a LCE effect does not exist.

In a recent MD study[43] we investigated the behavior of the scCH_4–CO_2 binary mixture with $X_{CH_4}=0.2$. The results obtained have shown that the nonpolar and non-HB CH_4 cosolvent does not form any aggregate in the mixture and the CH_4 molecules are well segregated. This fact supports the beliefs that only polar and especially HB cosolvents form aggregates when solvated in scCO_2. Due to this phenomenon, such polar HB cosolvent-CO_2 mixtures induce the enhancement of the solubility of polar compounds in these binary mixtures in comparison to the pure scCO_2 solvent.

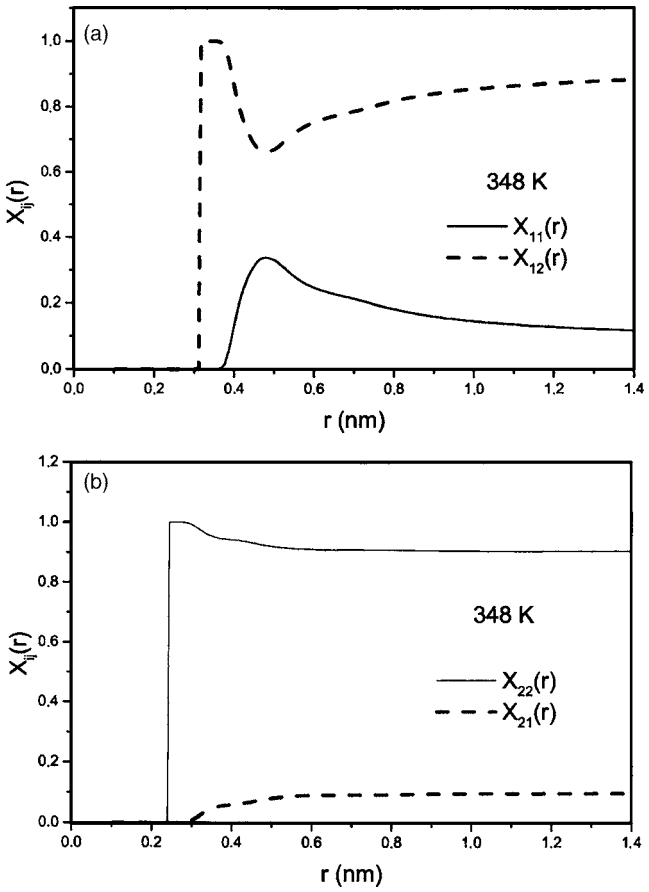

FIG. 4. (a) The calculated local mole fractions of EtOH and CO_2 around EtOH as a function of the intermolecular distance. (b) As in (a), but around CO_2.

In order to obtain a visual picture of these aggregation and LCE effects in the EtOH–CO_2 mixture, we depict in Fig. 5 a representative snapshot of the simulation box where only the EtOH molecules are displayed. From this figure the formation of EtOH aggregates in the mixture is clearly seen.

B. Dynamic properties

In addition to the static local intermolecular structure and LCE effects, we have also investigated the time dependent distribution of the local environment around the cosolvent and solvent molecules. The main purpose here is to study the effect of the local intermolecular structure (and LCE) around the EtOH molecules on the local environment reorganization dynamics, as well as on the single dynamic properties of the molecules in the fluid.

For this purpose, we have calculated the $C_{\delta n_{\mathrm{tot}(1)}}(t)\times(\mathrm{norm})$ and $C_{\delta n_{\mathrm{tot}(2)}}(t)(\mathrm{norm})$ ACFs [see Eqs. (8)–(10)], which correspond to the time behavior of the fluctuation of the total coordination number [Eqs. (6) and (7)] around the EtOH and CO_2 molecules (we recall here that indices 1 and 2 correspond to EtOH and CO_2, respectively) taking as cutoff distance for the coordination shell the first minimum of the EtOH–CO_2 COM PRDF (0.64 nm). These functions are shown in Fig. 6(a).

We may observe from these ACFs that they exhibit a very similar time behavior with the local density redistribu-

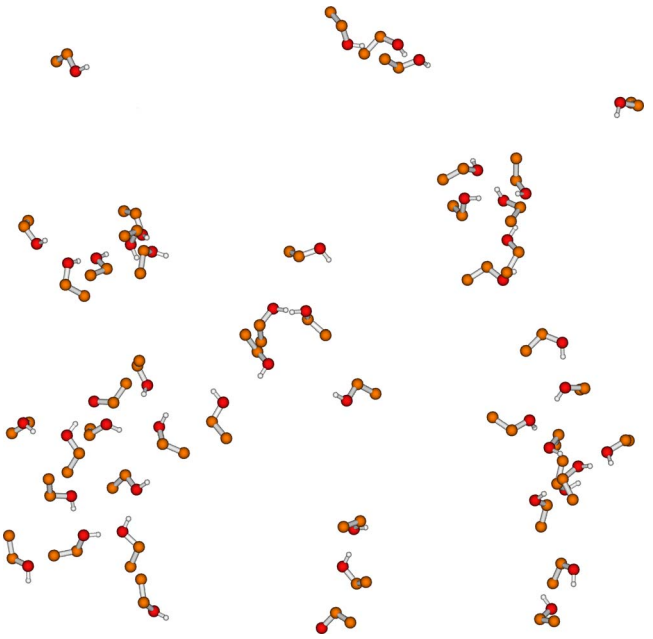

FIG. 5. (Color online) Representative snapshot of the simulation box, where only the EtOH molecules are displayed.

tion ACFs, $C_{\Delta\rho l}(t)$,[42,55] which we have been recently reported for several pure SCFs. We have pointed out[55] that the description of the dynamical behavior of the local environment around each molecule in a pure SCF involves two relaxation processes, namely, one responsible for the short-time dynamics and the other describing the long-time behavior. In particular, we found that a function consisting of two separate exponential decay functions might be proposed as the most appropriate one to interpret data for $C_{\Delta\rho l}(t)$,

$$C_{\Delta\rho l}(t) = C_1(t) + C_2(t) = ce^{-t/t_1} + (1-c)e^{-t/t_2}. \quad (12)$$

In the present treatment we have also found that this model function might be proposed as the most suitable one for the description of the characteristic features of the ACFs $C_{\delta n_{\mathrm{tot}(1)}}(t)$(norm) and $C_{\delta n_{\mathrm{tot}(2)}}(t)$(norm). Thus, using Eq. (12) we estimated the correlation times $\tau_{\delta n_{\mathrm{tot}(1)}}$ and $\tau_{\delta n_{\mathrm{tot}(2)}}$,

$$\tau_{\delta n_{\mathrm{tot}(1)}} = ct_1 + (1-c)t_2. \quad (13)$$

According to this procedure, the correlation times $\tau_{\delta n_{\mathrm{tot}(1)}}$ and $\tau_{\delta n_{\mathrm{tot}(2)}}$ are found to be 3.11 and 1.70 ps, respectively. The fitting parameter values for each ACF are also summarized in Table I. This significant difference between these correlation times reveals that the time required for the redistribution of the local environment around the EtOH cosolvent molecules is quite larger in comparison to the one corresponding to the local environment around CO_2. This retardation effect in the redistribution of the local environment of the EtOH cosolvent molecules is presumably caused by the EtOH aggregates, leading thus to a significant slowing down of local environment reorganization dynamics.

According to our previous studies concerning the local environment dynamics in pure SCFs,[42,55,63] as well as from studies concerning the contribution of attractive and repulsive interactions on solvation dynamics in SCFs,[60] the fast

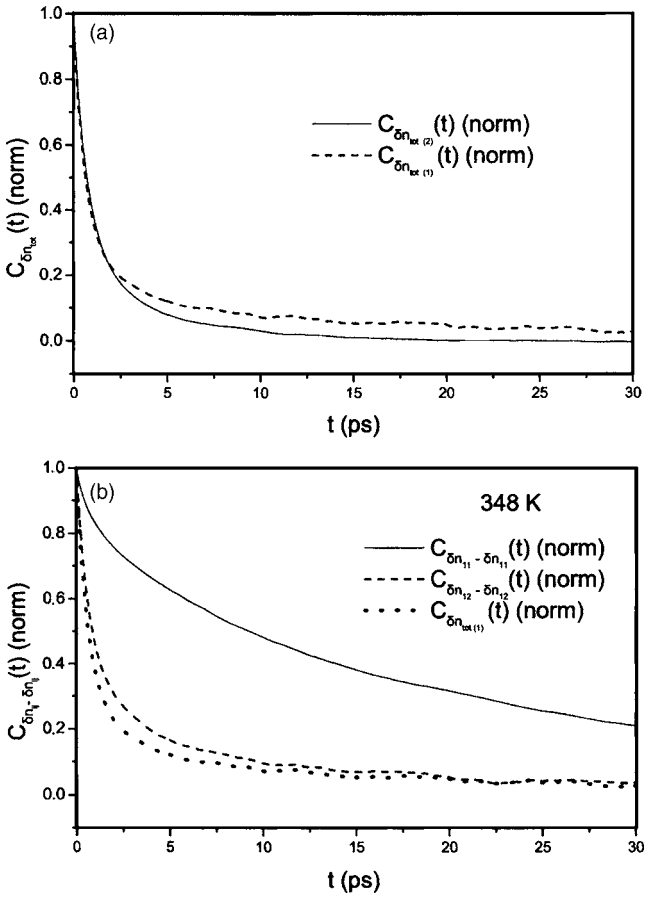

FIG. 6. (a) The calculated total $C_{\delta n_{\mathrm{tot}(1)}}(t)$(norm) and $C_{\delta n_{\mathrm{tot}(2)}}(t)$(norm) ACFs [Eqs. (8)–(10)] corresponding to the solvation shells of EtOH and CO_2, respectively. (b) The calculated $C_{\delta n_{11}\text{-}\delta n_{11}}(t)$(norm), $C_{\delta n_{12}\text{-}\delta n_{12}}(t)$(norm) and $C_{\delta n_{\mathrm{tot}(1)}}(t)$(norm) corresponding to the solvation shell of EtOH.

part of the local environment reorganization relaxation might be attributed to the repulsive interactions while the slow part was to the attractive ones. The fact that t_1, which characterizes the time decay of the slow part of the ACF, is significantly greater in the case of the solvation shell of EtOH (14.49 ps) in comparison with that of CO_2 (4.44 ps) supports this previous consideration.

To analyze further these results, we have calculated separately the ACFs $C_{\delta n_{11}\text{-}\delta n_{11}}(t)$(norm) and $C_{\delta n_{12}\text{-}\delta n_{12}}(t)\times$(norm) [Eq. (4)], which describe the time behavior of the fluctuation of the local coordination numbers of EtOH and CO_2 around EtOH, respectively. These two ACFs are displayed together with $C_{\delta n_{\mathrm{tot}(1)}}(t)$(norm) in Fig. 6(b). From Fig. 6(b) we observe that the decay of $C_{\delta n_{11}\text{-}\delta n_{11}}(t)$(norm) is sig-

TABLE I. Parameter values c, t_1, and t_2 obtained from the fits of the model function of Eq. (12) to the simulated $C_{\delta n_{\mathrm{tot}(1)}}(t)$(norm) and $C_{\delta n_{\mathrm{tot}(2)}}(t)\times$(norm) data for the specified solvation shells of scEtOH and $scCO_2$, respectively.

	c	t_1 (ps)	t_2 (ps)
$C_{\delta n_{\mathrm{tot}(1)}}(t)$(norm) (EtOH)	0.83	0.75	14.49
$C_{\delta n_{\mathrm{tot}(2)}}(t)$(norm) ($CO_2$)	0.74	0.74	4.44

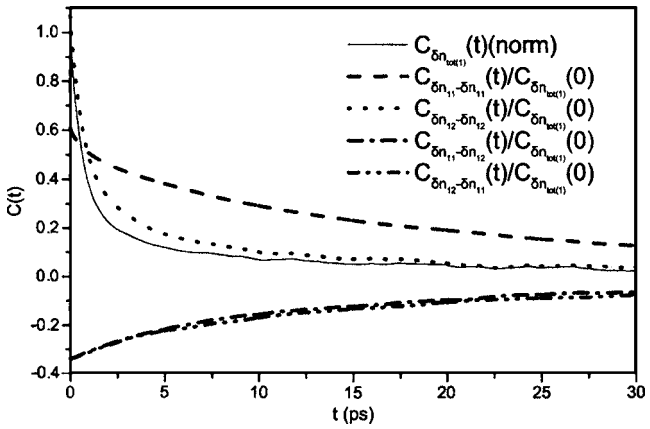

FIG. 7. The analysis of the total $C_{\delta n_{\mathrm{tot}(1)}}(t)$(norm) ACF in two autocorrelation and two cross-correlation functions.

nificantly slower in comparison to $C_{\delta n_{12}\text{-}\delta n_{12}}(t)$(norm) and $C_{\delta n_{\mathrm{tot}(1)}}(t)$(norm). This fact actually confirms our beliefs that the EtOH aggregates redistribute very slowly in time. Therefore, the time dependent redistribution of the solvation shell around the EtOH is mainly determined by the redistribution of the CO_2 molecules, as it is clearly seen in Fig. 6(b).

Further to this, the time dependent local environment around the EtOH molecules $C_{\delta n_{\mathrm{tot}(1)}}(t)$(norm) was analyzed in four separate component time correlation functions (TCFs), as it has been described in Sec. II and Eq. (10). The analysis of $C_{\delta n_{\mathrm{tot}(1)}}(t)$(norm) in two ACFs and two CCFS is depicted in Fig. 7. By inspecting carefully these results, we clearly observe that the time dependent distribution of the local environment around the EtOH molecules is mainly controlled by the time dependent distribution of the CO_2 molecules and that due to the cancellation effects between $C_{\delta n_{11}\text{-}\delta n_{11}}(t)$ and the sum of the CCFs $C_{\delta n_{11}\text{-}\delta n_{11}}(t)$ and $C_{\delta n_{12}\text{-}\delta n_{12}}(t)$. Moreover, the fast component of $C_{\delta n_{\mathrm{tot}(1)}}(t)$ $\times$(norm) is determined by the fast part of the ACF $C_{\delta n_{12}\text{-}\delta n_{12}}(t)$. Note that the decay of the ACF $C_{\delta n_{11}\text{-}\delta n_{11}}(t)$ and that of the CCFs $C_{\delta n_{11}\text{-}\delta n_{12}}(t)$ and $C_{\delta n_{12}\text{-}\delta n_{11}}(t)$ is mainly determined by one slow component and resembles that of a single exponential decay function. In other words, the strong attractive interactions between the EtOH molecules and (to lower extent) between EtOH–CO_2 predominate to the determination of the shape and decay of the TCFs $C_{\delta n_{11}\text{-}\delta n_{11}}(t)$, $C_{\delta n_{11}\text{-}\delta n_{12}}(t)$, and $C_{\delta n_{12}\text{-}\delta n_{11}}(t)$ leading thus to a very slow decay behavior of these correlations. It is very clear from Fig. 7 that $C_{\delta n_{12}\text{-}\delta n_{12}}(t)$ is mainly responsible for the reorganization of the local environment of EtOH, for a length scale of the order of the EtOH–CO_2 first solvation shell radius.

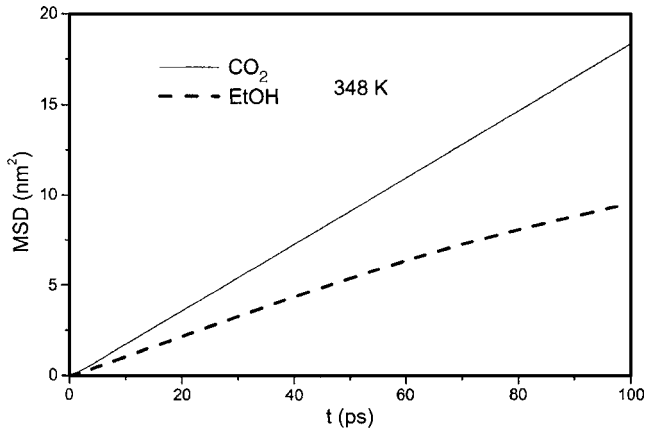

FIG. 8. The calculated mean square displacements for EtOH and CO_2 molecules in the mixture as a function of time.

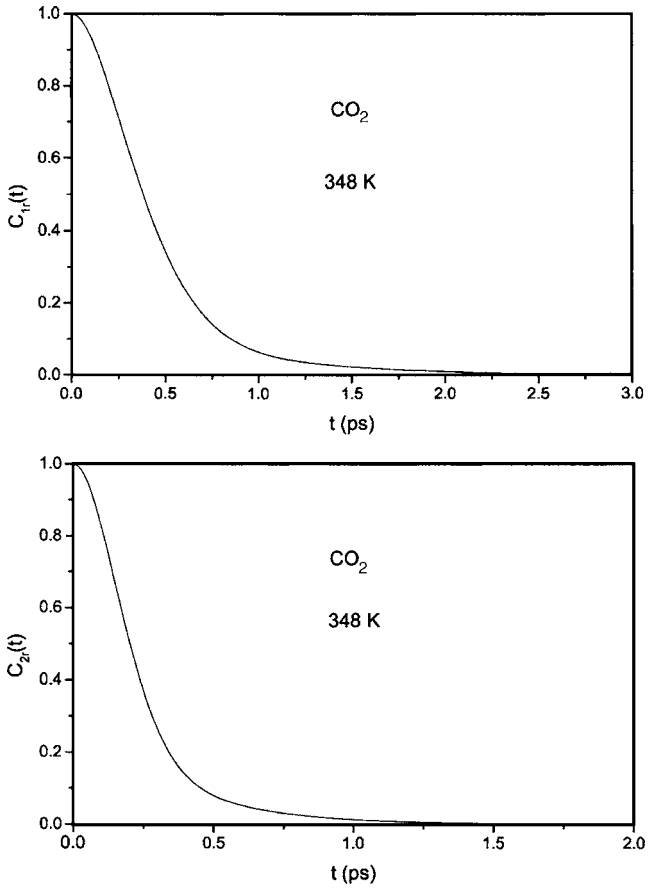

FIG. 9. The calculated reorientational ACFs $C_{1r}(t)$ and $C_{2r}(t)$ for CO_2 in the mixture.

All the above features obtained indicate that the redistribution of the CO_2 molecules in the solvation shell of EtOH is significantly faster than that to the EtOH molecules and determines significantly the time dependent local environment reorganization, since the EtOH aggregates due to the strong attractive HB interactions dissociate quite slowly.

In addition, we calculated the self-diffusion coefficients of EtOH and CO_2 molecules by using the mean square displacements (MSDs) of the particles in the fluid. The average MSD for EtOH and CO_2 is depicted in Fig. 8 and according to the Einstein relation the calculated self-diffusion coefficients are $D_{CO_2}=30.81\times10^{-9}$ m^2 s^{-1} and $D_{EtOH}=13.17\times10^{-9}$ m^2 s^{-1}. Although the EtOH and CO_2 molecules have about similar masses, the self-diffusion coefficient of CO_2 is significantly larger and this fact signifies that the aggregation between the EtOH particles affects strongly their translational dynamic behavior. A similar behavior has been also pointed out for the sc MeOH–CO_2 binary mixture by recent MD simulations of our group,[25] supported by NMR spin echo measurements,[27] signifying thus the effect of the alcohol aggregation upon their translation dynamics.

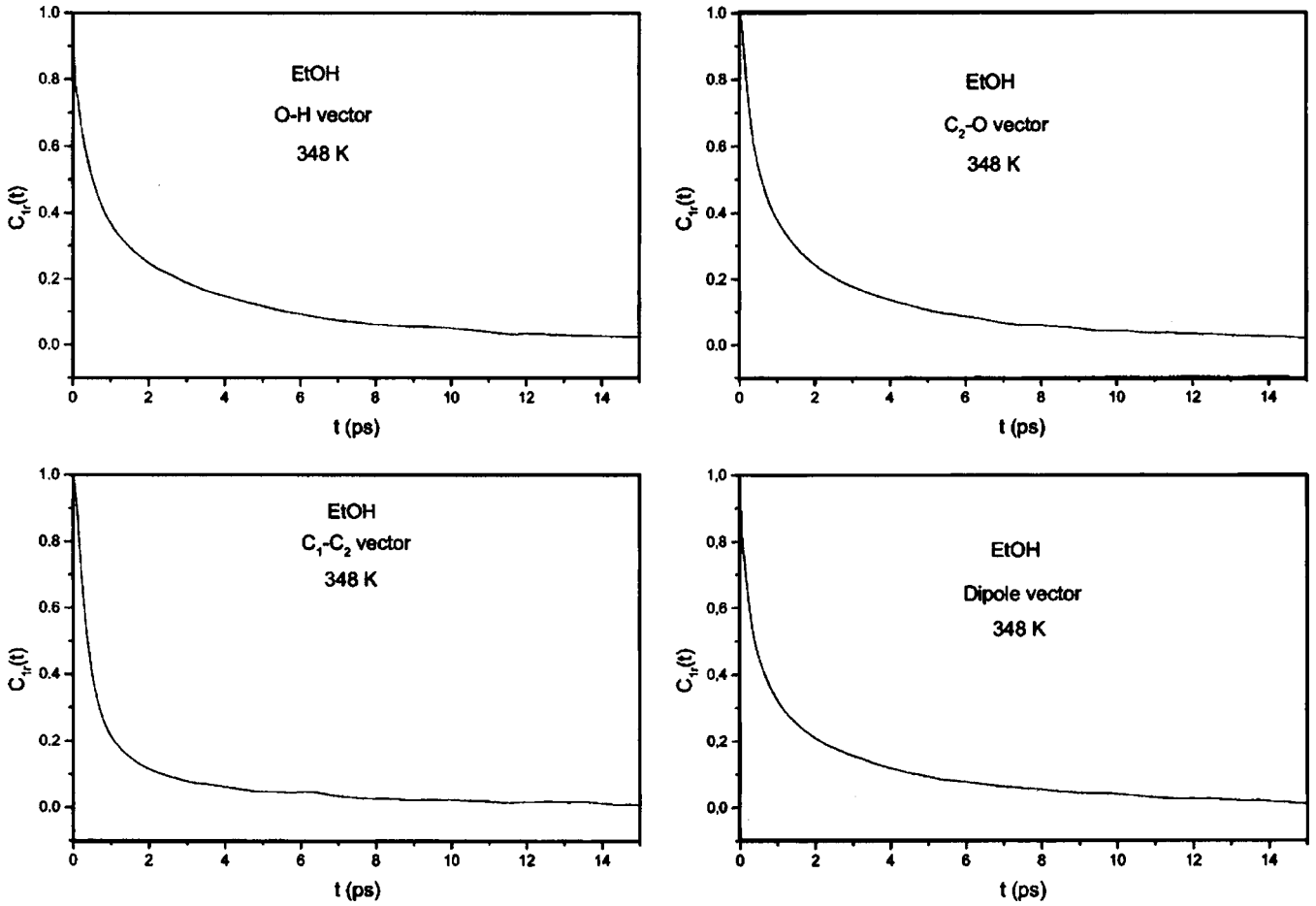

FIG. 10. The various calculated reorientational ACFs $C_{1r}(t)$ for EtOH in the mixture.

To explore systematically for a possible interrelation between the local environment and single-molecule dynamics, we have also investigated the single reorientational dynamics of both types of particles in the fluid. In this case, we investigated the single reorientational dynamics as usual by means of the Legendre ACFs. In the case of CO_2 we have used a unit vector along the C–O axis. For EtOH we used the unit vectors along the C_1-C_2, C_2-O, O–H, and the molecular dipole axis.

The Legendre reorientational ACFs are defined by the well-known relation,

$$C_{lr}(t) = \langle P_l(\mathbf{u}(0) \cdot \mathbf{u}(t)) \rangle, \quad l = 1,2. \tag{14}$$

The corresponding first and second order Legendre reorientational ACFs for the CO_2 and EtOH molecules are depicted in Figs. 9–11. Furthermore, their calculated reorientational correlation times τ_{1r}, and τ_{2r} are presented in Table II. We can see that the time decay of the reorientational ACFs of EtOH is significantly slower in comparison to CO_2. In addition, the τ_{1r} and τ_{2r} values obtained for EtOH are also significantly larger in comparison to those obtained for CO_2. This fact indicates that the alcohol aggregation affects not only the EtOH single translational dynamics, but also their reorientational dynamic behavior.

By comparing the τ_{1r} and τ_{2r} values for the O–H and the molecular dipole vector of EtOH in the mixture with those for pure liquid[61] and scEtOH (Ref. 45) at comparable densities, we may conclude that τ_{1r} and τ_{2r} in the mixture are lower in comparison to those corresponding to the pure liquid but higher than those at sc conditions. Additionally the C_1-C_2, C_2-O, O–H, and molecular dipole vector Legendre ACFs of EtOH are different to each other, an observation which comes in agreement with our previous finding concerning the C–O and O–H reorientational dynamics in pure scMeOH (Ref. 55) and scEtOH.[45] In other words, this means that the local environment differently affects the reorientational dynamics of each specific intramolecular bond vector. It also explains why the correlation times τ_{1r} and τ_{2r} of the O–H vector are greater than those corresponding to the C_1-C_2, C_2-O, and molecular dipole vectors, since they are more strongly affected by the microscopic local HB network around the EtOH molecules. Moreover, the well-known Hubbard relation is not fulfilled, indicating thus that the reorientational motions of the EtOH molecules could not be characterized as diffusive. This is also clearly seen from Figs. 10 and 11, where we may observe that the time decay of $C_{1r}(t)$ and $C_{2r}(t)$ for all the bond vectors of EtOH could not be well represented by a single exponential decay model function.

In the case of the reorientational ACFs and the corresponding correlation times of CO_2, they have been found to be quite similar with those for pure $scCO_2$ obtained by the MD simulations of our group,[55] as well as by previously reported NMR measurements[62] at comparable conditions. For example, at $T=351.4$ K and a density $\rho=0.618$ g/cm^3

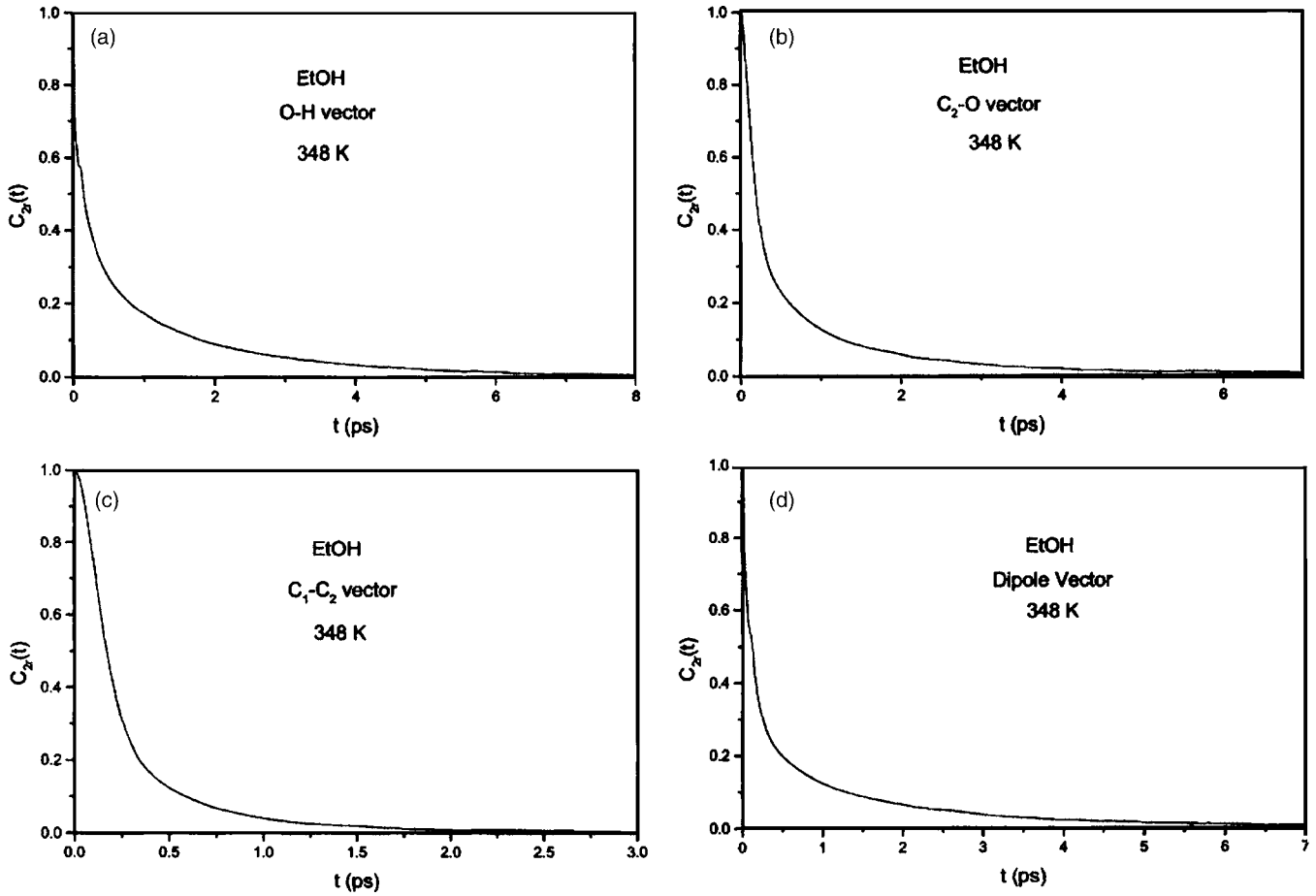

FIG. 11. The various calculated reorientational ACFs $C_{2r}(t)$ for EtOH in the mixture.

the experimental value of τ_{2r} is 0.245 ps, whereas in our case the simulated value of τ_{2r} is 0.252 ps (Table II). This fact actually reveals that the single dynamic properties of the CO_2 molecules are not affected by the addition of the EtOH cosolvent molecules. This behavior of CO_2 has been also revealed for the $scCO_2-CH_4$ mixture[43] from MD simulation studies.

IV. CONCLUDING REMARKS

The molecular dynamics simulation technique was employed to investigate the features concerning the LCE effects and related dynamics in the CO_2-ethanol binary mixed solvents, with ethanol acting as cosolvent. The methodology employed to estimate these properties was based on the calculation of the pair radial distribution functions, local coordination numbers, and the corresponding local mole fractions around the CO_2 and EtOH molecules in the fluid. The time evolution of the local environment around the CO_2 and EtOH molecules in the mixture was also investigated. This was achieved by calculating the appropriate time correlation functions of the deviation of the local coordination numbers relative to the mean ones and the corresponding correlation times introduced in Ref. 63 and presented here.

TABLE II. The calculated reorientational correlation times τ_{1r} and τ_{2r} for several intramolecular axes of scEtOH and CO_2.

CO_2	C–O axis			
τ_{1r} (ps)	0.47			
τ_{2r} (ps)	0.25			
EtOH	O–H axis	C_2-O axis	C_1-C_2 axis	Dipole axis
τ_{1r} (ps)	1.93	1.90	1.11	1.63
τ_{2r} (ps)	0.65	0.53	0.28	0.50

The estimated average local coordination numbers and mole fractions around the species in the mixture have revealed the existence of local composition enhancement of EtOH around the EtOH cosolvent molecules. This result clearly indicates the nonideal mixing behavior of the mixture and the existence of hydrogen-bonded aggregates between the ethanol molecules.

Generally, the results obtained reveal that the time required for the redistribution of the local environment around the EtOH cosolvent molecules is quite larger in comparison to the one corresponding to the redistribution of the local environment around CO_2. This retardation effect in the redistribution of the local environment of the EtOH cosolvent molecules is presumably caused by the formation of aggregates between the EtOH molecules, leading in this way to a significant slowing down of local environment dynamics.

Furthermore, the analysis of the obtained ACF of the total local coordination number of EtOH in four separate components, namely, two autocorrelation functions and two cross-correlation ones, has revealed that the time dependent

reorganization of the local environment around EtOH is mainly determined by the reorganization of the CO_2 molecules, due to the existence of cancellation effects.

Finally, the single-molecule translational and reorientational dynamics have been investigated and the results obtained indicate a possible interrelation between the single-molecule and local environment dynamics of EtOH, signifying the effect of EtOH aggregation upon the translational and reorientational dynamics of the EtOH molecules.

ACKNOWLEDGMENTS

This work was carried out within the Project No. 70/3/8371 (Greece-Russia: Joint Research and Technology Programme) founded by the Greek Secretariat of Research and Technology (GSRT)-Ministry of Development. The computer time allocation on the facilities of the Computer Center of the National and Kapodistrian University of Athens is also gratefully acknowledged.

[1] K. P. Johnston, S. Kim, J. Coumbes, and J. M. L. Penninger, *Supercritical Fluid Science and Technology* (American Chemical Society, Washington, 1998), Chap. 5 and references therein.
[2] S. C. Tucker, Chem. Rev. (Washington, D.C.) **99**, 391 (1999).
[3] O. Kajimoto, Chem. Rev. (Washington, D.C.) **99**, 355 (1999).
[4] C. A. Eckert, B. L. Knutson, and P. G. Debenedetti, Nature (London) **383**, 313 (1996).
[5] E. Kiran and J. M. H. Levelt Sengers, in *Supercritical Fluids: Fundamentals for Application*, NATO Advanced Study Institute, Series E: Applied Science Vol. 273, edited by J. M. H. Levelt Sengers and M. H. Johanna, (Kluwer Academic, Dordrecht, 1994).
[6] N. Akiya and P. Savage, Chem. Rev. (Washington, D.C.) **102**, 2725 (2002).
[7] M. Besnard, T. Tassaing, Y. Danten, J. M. Andanson, J. C. Soetens, F. Cansell, A. Loppinet-Serani, H. Reveron, and C. Aymonier, J. Mol. Liq. **125**, 88 (2006).
[8] X. Zhang, B. Han, Z. Hou, J. Zhang, Z. Liu, T. Jiang, J. He, and H. Li, Chem.-Eur. J. **8**, 5107 (2002).
[9] S. Sala, T. Tassaing, N. Ventosa, Y. Danten, M. Besnard, and J. Veciana, ChemPhysChem **5**, 243 (2004).
[10] J. M. Dobbs, J. M. Wong, R. J. Lahiere, and K. P. Johnston, Ind. Eng. Chem. Res. **26**, 56 (1987).
[11] R. M. Lemert and K. P. Johnston, Ind. Eng. Chem. Res. **30**, 1222 (1991).
[12] G. S. Gurdial, S. J. Macnaughton, D. L. Tomasko, and N. R. Foster, Ind. Eng. Chem. Res. **32**, 1488 (1993).
[13] B. Guan, Z. Liu, B. Han, and Y. Han, J. Supercrit. Fluids **14**, 213 (1999).
[14] Y. Koga, Y. Iwai, Y. Hata, M. Yamamoto, and Y. Arai, Fluid Phase Equilib. **125**, 115 (1996).
[15] M. Roth, J. Chromatogr., A **1037**, 369 (2004).
[16] C. Boukouvalas, K. Magoulas, and D. Tassios, Sep. Sci. Technol. **33**, 387 (1998).
[17] Z. Huang, Y. C. Chiew, W.-D. Lu, and S. Kawi, Fluid Phase Equilib. **237**, 9 (2005).
[18] H.-K. Bae, J.-H. Jeon, and H. Lee, Fluid Phase Equilib. **222–223**, 119 (2004).
[19] P. Lalanne, S. Rey, F. Cansell, T. Tassaing, and M. Besnard, J. Supercrit. Fluids **19**, 199 (2001).
[20] T. Tassaing, P. Lalanne, S. Rey, F. Cansell, and M. Besnard, Ind. Eng. Chem. Res. **39**, 4470 (2000).
[21] J. Chen, D. Shen, W. Wu, B. Han, B. Wang, and D. Sun, J. Chem. Phys. **122**, 204508 (2005).
[22] S. Kim and K. P. Johnston, AIChE J. **33**, 1603 (1987).
[23] D. J. Philips and J. F. Brennecke, Ind. Eng. Chem. Res. **32**, 943 (1993).
[24] S. P. Kelley and R. M. Lemert, AIChE J. **42**, 2047 (1996).
[25] G. Chatzis and J. Samios, Chem. Phys. Lett. **374**, 187 (2003).
[26] (a) J. M. Stubbs and J. I. Siepmann, J. Chem. Phys. **121**, 1525 (2004); (b) H. Li and M. Maroncelli, J. Phys. Chem. B **110**, 21189 (2006).
[27] H. D. Lüdemann and L. Chen, J. Phys.: Condens. Matter **14**, 11453 (2002).
[28] J. L. Fulton, G. G. Yee, and R. D. Smith, J. Am. Chem. Soc. **113**, 8327 (1991).
[29] D. M. Pfund, J. L. Fulton, and R. D. Smith, in *Aggregation of MeOH in Supercritical Fluids. A Molecular Dynamics Study*, Supercritical Fluid Engineering Science Fundamentals and Applications, ACS Symposium Series Vol. 514, edited by J. F. Brennecke and E. Kiran (American Chemical society, Washington, DC, 1993).
[30] J. L. Fulton, G. G. Yee, and R. D. Smith, in *Hydrogen Bonding of Simple Alcohols in Supercritical Fluids*, Supercritical Fluid Engineering Science Fundamentals and Applications, ACS Symposium Series Vol. 514, edited by J. F. Brennecke and E. Kiran (American Chemical Society, Washington, DC, 1993).
[31] C. M. V. Taylor, S. Bai, C. L. Mayne, and D. M. Grant, J. Phys. Chem. B **101**, 5652 (1997).
[32] M. Kanakubo, T. Aizawa, T. Kawakami, O. Sato, Y. Ikushima, K. Hatakeda, and N. Saito, J. Phys. Chem. B **104**, 2749 (2000).
[33] D. L. Goldfarb, D. P. Fernandez, and H. R. Corti, Fluid Phase Equilib. **158**, 1011 (1999).
[34] R. L. Smith, C. Saito, S. Suzuki, S. B. Lee, H. Inomata, and K. Arai, Fluid Phase Equilib. **194**, 869 (2002).
[35] D. S. Bulgarevich, T. Sato, T. Sugeta, K. Otake, M. Sato, M. Uesugi, and M. Kato, J. Chem. Phys. **108**, 3915 (1998).
[36] P. Lalanne, T. Tassaing, Y. Danten, F. Cansell, S. C. Tucker, and M. Besnard, J. Phys. Chem. A **108**, 2617 (2004).
[37] H. Pöhler and E. Kiran, J. Chem. Eng. Data **42**, 384 (1997).
[38] G. S. Gurdial, N. R. Foster, S. L. J. Yun, and K. D. Tilly, in *Phase Behavior of Supercritical Fluid Entrainer Systems*, Supercritical Fluid Engineering Science Fundamentals and Applications, ACS Symposium Series Vol. 514, edited by J. F. Brennecke and E. Kiran (American Chemical Society, Washington, DC, 1993).
[39] X. Zhang, B. Han, L. Shi, H. Li, and G. Yang, J. Supercrit. Fluids **24**, 193 (2002).
[40] K. D. Tilly, N. R. Foster, S. J. Macnaughton, and D. L. Tomasko, Ind. Eng. Chem. Res. **33**, 681 (1994).
[41] M. Saharay and S. Balasubramanian, J. Phys. Chem. B **110**, 3782 (2006).
[42] I. Skarmoutsos and J. Samios, J. Phys. Chem. B **110**, 21931 (2006).
[43] I. Skarmoutsos and J. Samios, J. Mol. Liq. **125**, 181 (2006).
[44] I. Skarmoutsos, L. I. Kampanakis, and J. Samios, J. Mol. Liq. **117**, 33 (2005).
[45] D. Dellis, M. Chalaris, and J. Samios, J. Phys. Chem. B **109**, 18575 (2005).
[46] M. Chalaris and J. Samios, J. Phys. Chem. B **103**, 1161 (1999).
[47] S. Marinakis and J. Samios, J. Supercrit. Fluids **34**, 81 (2005).
[48] M. W. Maddox, G. Goodyear, and S. C. Tucker, J. Phys. Chem. B **104**, 6266 (2000).
[49] L. Zhang and J. I. Siepmann, Theor. Chem. Acc. **115**, 391 (2006).
[50] Y. Tian, L. Chen, M. Li, and H. Fu, J. Phys. Chem. A **107**, 3076 (2003).
[51] J. M. Ziegler, T. L. Chester, D. P. Innis, S. H. Page, and J. G. Dorsey, in *Innovations in Supercritical Fluids*, ACS Symposium Series Vol. 608, edited by K. W. Hutchinson and N. R. Foster (American Chemical Society, Washington, DC, 1996).
[52] J. G. Harris and K. H. Young, J. Phys. Chem. **99**, 12021 (1995).
[53] W. L. Jorgensen, J. Phys. Chem. **90**, 1276 (1986).
[54] J. E. Adams and A. Siavosh-Haghighi, J. Phys. Chem. B **106**, 7973 (2002).
[55] I. Skarmoutsos and J. Samios, J. Chem. Phys. **126**, 044503 (2007).
[56] H. J. C. Berendsen, J. P. M. Postma, W. F. van Gunsteren, A. DiNola, and J. R. Haak, J. Chem. Phys. **81**, 3684 (1984).
[57] J. P. Ryckaert, G. Ciccotti, and H. J. C. Berendsen, J. Comput. Phys. **23**, 327 (1977).
[58] M. P. Allen and D. J. Tildesley, *Computer Simulation of Liquids* (Oxford University Press, Oxford, 1987).
[59] D. Paschek and A. Geiger, MOSCITO 4.1, University of Dortmund, Dortmund, Germany, 2003.
[60] T. Yamaguchi, Y. Kimura, and N. Hirota, J. Chem. Phys. **111**, 4169 (1999).
[61] L. Saiz, J. A. Padro, and E. Guardia, J. Phys. Chem. B **101**, 78 (1997).
[62] T. Umecky, M. Kanakubo, and Y. Ikushima, J. Phys. Chem. B **107**, 12003 (2003).
[63] I. Skarmoutsos, Ph.D. thesis, National and Kapodistrian University of Athens, 2006.